Effect of chlorine group position on adsorption behavior and corrosion inhibition of Chlorobenzylideneamino-5-methyl-2, 4-dihydro-1, 2, 4-triazole-3-thione Schiff bases: Experimental study

M. Larouj[(a)(b)], H. Lgaz[(a)(b)], R. Salghi[(b)]*, S. Jodeh[(c)], M. Messali[(d)], M. Zougagh[(e)(f)], H.Oudda[(a)] , A. Chetouani[(g)]

[(a)] *Laboratory of Separation Processes, Central Post133, Kenitra , Faculty of Sciences, University IbnTofail, Morocco.*

[(b)] *Laboratory of Applied Chemistry and Environment, ENSA, Université Ibn Zohr,PO Box 1136, 80000 Agadir, Morocco*

[(c)] *Department of Chemistry, An-Najah National University, P. O. Box 7, Nablus, Palestine*

[(d)]*Chemistry Department, Faculty of Science, Taibah University, 30002, Al-Madinah Al-Mounawwara, Saudi Arabia.*

[(e)]*Regional Institute for Applied Chemistry Research, IRICA, E-13004, Ciudad Real, Spain*

[(f)] *Castilla-La Mancha Science and Technology Park, E-02006, Albacete, Spain*

[(g)] *Laboratoire de Chimie Appliquée et environnement (LCAE-URAC18), Faculté des Sciences, 60000 Oujda, Morocco.*

* Corresponding author. E-mail (R. Salghi): r.salghi@uiz.ac.ma

Abstract

The corrosion inhibition and adsorption of 4-(n-Chlorobenzylideneamino)-5-methyl-2,4-dihydro-1,2,4-triazole-3-thione (n-CBAT) Schiff bases has been investigated on steel electrode in 1.0 M HCl by using weight loss, potentiodynamic polarization curves, and electrochemical impedance spectroscopy (EIS) methods. The results show that all n-CBAT are good inhibitors, and inhibition efficiency follows the order:**4-CBAT <3-CBAT <2-CBAT**. Polarization curves reveal that all studied inhibitors are mixed type. The adsorption of each inhibitor on mild steel surface obeys Langmuir adsorption isotherm. EIS spectra exhibit one capacitive loop and confirm the inhibitive ability. The effect of temperature on the corrosion behavior with addition of 1×10^{-3}Mof **n-CBAT** added was studied in the temperature range 30–60∘C. The thermodynamic parameters activation were determined and discussed.

Keywords: *Carbon steel; Corrosion inhibition; Schiff bases; Triazole; Electrochemical techniques.*

1. Introduction

Acid solutions with pH values below one are generally used for industrial acid cleaning, acid descaling, the pickling, oil well acidizing and removal of undesirable rust [1–3]. Mild steel which are extensively used in a

lot of industrial processes, could corrode during these acidic applications particularly with the use of HCl [4, 5]. Corrosion prevention systems favor the use of corrosion inhibitors with low or zero environmental impacts. Inhibitors are chemicals that react with a metallic surface or the environment. Inhibitors decrease corrosion processes by increasing the anodic or cathodic polarization behavior, reducing the movement or diffusion of ions to the metallic surface and increasing the electrical resistance of the metallic surface [6]. The use of organic molecules as corrosion inhibitors is one of the most practical methods for protecting against the corrosion and it's becoming increasingly popular. These compounds in general are adsorbed on the metal surface and blocking the active corrosion sites. Four types of adsorption may take place by organic molecules at metal/solution interface:

- ✓ Interaction of π-electrons with the metal
- ✓ Interaction of unshared electron pairs in the molecule with the metal
- ✓ Electrostatic attraction between the charged molecules and the charged metal
- ✓ Combination of (a) and (c)

The choice of an appropriate inhibitor depends on the physicochemical properties of the inhibitor molecule, the nature and state of the metal surface, and the type of the corrosion medium. Inhibitors have been selected mainly by using empirical knowledge based on their macroscopic physicochemical properties. Recently, the effectiveness of an inhibitor molecule has been related to its spatial as well as its electronic structure [7-10].

In the literature, several Schiff bases have reported as effective corrosion inhibitors for different metals and alloys in acidic media [11–14]. Increasing popularity of Schiff bases in the field of corrosion inhibition science based on the ease of synthesis from relatively inexpensive starting materials and their eco-friendly or low toxic properties [15, 16]. Due to the presence of the -C = N- group, electronegative nitrogen, sulfur and/or oxygen atoms in the molecule, Schiff bases should be good corrosion inhibitors. The action of such inhibitors depends on the specific interaction between the functional groups and the metal surface [17, 18]. These molecules normally form a very thin and persistent adsorbed film that lead to decrease in the corrosion rate due to the slowing down of anodic, cathodic reaction or both [19,20]. The objective of this work is to present the relationships between the Schiff bases reactivity and their ability to inhibit the corrosion of mild steel in hydrochloric acid to understand if any structural differences induced by different positions of the chlorine group may be related to the experimentally observed differences of corrosion efficiency.

2. Experimental

2.1. Materials preparation

The steel used in this study is a carbon steel had the following composition (atom %):0.370 % C, 0.230 % Si, 0.680 % Mn, 0.016 % S, 0.077 % Cr, 0.011 % Ti, 0.059 % Ni, 0.009 % Co, 0.160 % Cu and the remainder iron (Fe).The metal specimens used in weight loss studies have a rectangular form (length = 1.6 cm, width = 1.6 cm, thickness = 0.07 cm).For electrochemical studies, same type of coupons was used but only 1 cm^2 area was exposed during each measurement. Before measurements the samples were polished using different grades of emery papers SiC (120, 600 and 1200); and then subjected to the action of a buffing machine attached with a cotton wheel and a fiber wheel having buffing soap to ensure mirror bright finish, degreased by washing with ethanol, acetone and finally washed with distilled water. The aggressive solutions of 1.0 M HCl were prepared by dilution of analytical grade 37% HCl with distilled water. The concentration range of compounds of the Schiff bases used was 1×10^{-6}M to 1×10^{-3}M.

2.2. Inhibitor synthesis

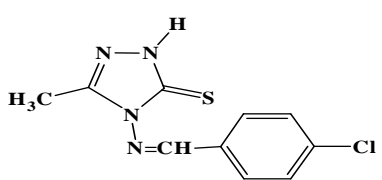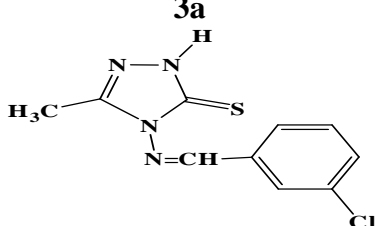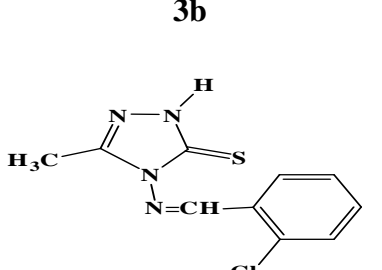General procedure for the Synthesis of4-(arylideneamino)-5-methyl-2,4-dihydro-1,2,4-triazole-3-thione derivatives.

Scheme: An easy, fast, and cheap way for the synthesis of the new Schiff bases derivatives.

(**1**) 4-amino-5-methyl-2,4-dihydro-1,2,4-triazole-3-thione.

(**2**) Substituted benzaldehyde.

(**3a-c**) 4-(arylideneamino)-5-methyl-2,4-dihydro-1,2,4-triazole-3-thione derivatives.

Table1: The chemical structure and IUPAC name of the Schiff bases.

Compound structure	name
3a	4-(4-Chlorobenzylideneamino)-5-methyl-2,4-dihydro-1,2,4-triazole-3-thione **4-CBAT**
3b	4-(3-Chlorobenzylideneamino)-5-methyl-2,4-dihydro-1,2,4-triazole-3-thione **3-CBAT**
3c	4-(2-Chlorobenzylideneamino)-5-methyl-2,4-dihydro-1,2,4-triazole-3-thione **2-CBAT**

2.3. Measurements

2.3.1. Weight loss measurements

Carbon steel specimens were accurately weighed and then immersed in 1.0 M HCl solutions without and with inhibitors for 6 h. After that, the specimens were withdrawn and carefully cleaned by distilled water

and acetone, and then dried and weighed. Triplicate experiments were performed in each case and the mean value of the weight loss was calculated.

2.3.2. Electrochemical measurements

Electrochemical tests were carried out in a conventional three electrode cell with platinum counter electrode, saturated calomel electrode as the reference electrode and the carbon steel with the surface area of 1 cm^{2}as the working electrode.Electrochemical experiments were conducted using impedance equipment (Tacussel Radiometer PGZ 100) and controlled with Tacussel corrosion analysis software model Voltamaster 4.

Before electrochemical tests, the working electrode was immersed in test solution at open circuit potential (OCP) for 30 min to attain a stable state. In order to minimize ohmic contribution, the tip of lugging capillary was kept close to working electrode. The potential of potentiodynamic polarization curves started from potential -800 mV to -200 mV vs. SCE with a scan rate of 1 mV s^{-1}. Electrochemical impedance spectroscopic studies were carried out at OCP in the frequency range of 10 mHz - 100 kHz, with 10 points per decade, at the rest potential, after 30 min of acid immersion, by applying 10 mV peak to peak voltage excitation. Nyquist plots were made from these experiments. The best semicircle can be fit through the data points in the Nyquist plot using a non-linear least square fit so as to give the intersections with the *x*-axis.

3. Results and discussion

3.1. Potentiodynamic polarization measurements

Figs. 1a-c shows representative Tafel polarization curve of steel in 1.0M HCl solution in the presence of different concentrations of compounds of the Schiff bases. According to these Figures, lower corrosion current was obtained for 2-CBAT and therefore 2-CBAT is more beneficial rather than 3-CBAT and 4-CBAT. Table 2shows the electrochemical corrosion kinetic parameters such as corrosion potential (E$_{corr}$ vs. SCE), corrosion current density (I$_{corr}$), cathodic Tafel slope (β_c) and inhibition efficiency (η_{Tafel}) obtained by extrapolation of the Tafel lines for inhibitors. The inhibition efficiency for different concentrations of inhibitor is calculated using the following equation [21, 22]:

$$\eta_{Tafel}(\%) = \frac{I_{corr} - I_{corr(i)}}{I_{corr}} \times 100 \tag{1}$$

Where I_{corr} and $I_{corr(i)}$are the corrosion current densities determined by the intersection of the extrapolated Tafel lines and the corrosion potential for steel in uninhibited and inhibited acid solution, respectively.

As was expected both anodic and cathodic reactions of steel electrode corrosion were inhibited with the increase of the inhibitors concentration. This result suggests that the addition of the inhibitors reduces anodic dissolution and also retards the hydrogen evolution reaction [23]. The electrochemical processes on the metal surface are related to the adsorption of the inhibitors and the adsorption is known to depend on the chemical structure of the inhibitors. The parallel cathodic Tafel curves in Figs.1a-c and the values of β_c in table 2show that the hydrogen evolution is activation-controlled and the reduction mechanism is not affected by the presence of the inhibitors. We can classify an inhibitor as cathodic or anodic type if the displacement in corrosion potential is more than 85 mV with respect to corrosion potential of the blank [24]. In the presence of the Schiff base inhibitors, the corrosion potential of carbon steel shifted to the negative side only 20 mV (vs. SCE), suggesting that these compounds behave as mixed-type inhibitors [25]. However, the

influence is more pronounced in the cathodic polarization plots compared to that in the anodic polarization plots. It is clear that the addition of the inhibitor shifts the cathodic curves to a greater extent toward the lower current density when compared to the anodic curves. The E_{corr} value is also shifted to the more negative side with an increase in the inhibitor concentration [26]. It can be seen that the corrosion rate decreased and inhibition efficiency (η_{Tafel} (%)) increased by increasing inhibitors concentration. The higher concentration of inhibitors provides better inhibition efficiency. The results show that 4-CBAT is good inhibitor, and inhibition efficiency follows the order: **4-CBAT <3-CBAT <2-CBAT**.
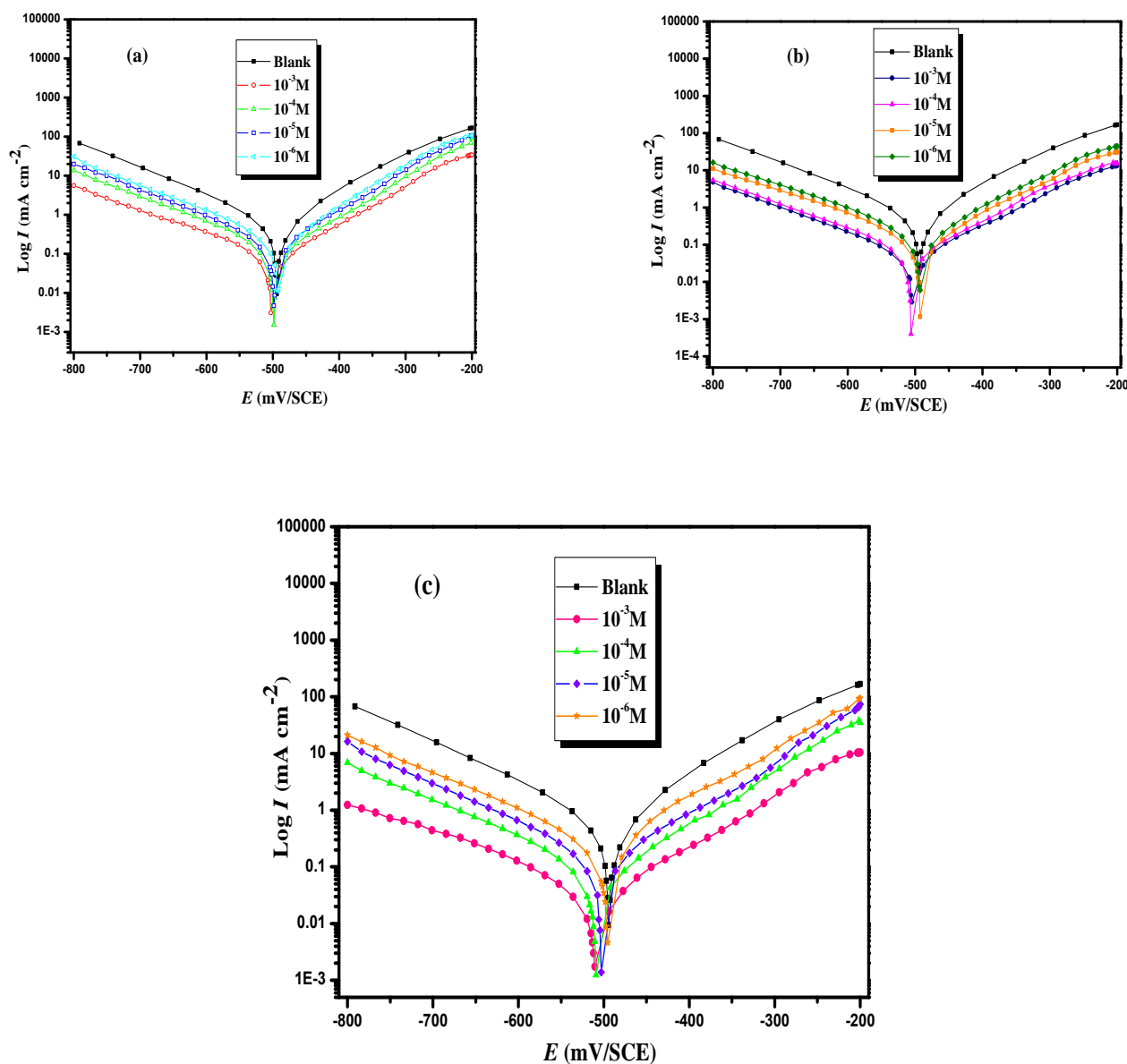
Fig.1. Polarisation curves of carbon steel in 1.0MHClfor various concentrations of the inhibitors: (a) 4-CBAT, (b) 3-CBAT, (c) 2-CBAT 303K.

Table2. Electrochemical parameters of carbon steel at various concentrations of n-CBAT inhibitors in 1.0M HCl. and corresponding inhibition efficiency.

Inhibitor	Conc (M)	$-E_{corr}$ (mV/SCE)	$-\beta c$ (mV dec^{-1})	I_{corr} (mA cm^{-2})	η_{Tafel} (%)
Blank	1.0	496	150.0	564	--------
4-CBAT	10^{-3}	504	155.4	**67.08**	**87.11**
	10^{-4}	502	158.5	162.04	71.27
	10^{-5}	500	149.0	195.59	65.32
	10^{-6}	495	158.0	272.02	51.77
3-CBAT	10^{-3}	515	160.6	**55.05**	**90.24**
	10^{-4}	509	158.7	100.67	82.15
	10^{-5}	495	162.6	146.58	74.01
	10^{-6}	495	156.3	235.81	58.19
2-CBAT	10^{-3}	512	157.1	**24.03**	**94.20**
	10^{-4}	512	162.1	73.26	87.01
	10^{-5}	505	151.2	134.35	76.18
	10^{-6}	498	157.3	218.36	61.23

*3.2. Electrochemical impedance spectroscopy*

The corrosion of carbon steel in 1.0 M HCl solution in the presence of of the Schiff base inhibitorswas investigated by EIS at 303K after an exposure period of 30 min. Nyquist plots for carbon steel obtained at the interface in the absence and presence of this inhibitor at different concentrations is given in Fig.2a-c.

Figs2a-c show Nyquist plots for steel in 1.0 M HCl solution in the presence of different concentrations of the Schiff base inhibitors. The plots show a depressed capacitive loop which arises from the time constant of the electrical double layer and charge transfer resistance. As can be seen, higher charge transfer resistance was obtained in presence of **2-CBAT**.The impedance of the inhibited steel increases with increasing the inhibitor's concentration and consequently the inhibition efficiency increases. The equivalent circuit compatible with the Nyquist diagram recorded in the presence of inhibitors was depicted in Fig. 3.

The simplest approach requires the theoretical transfer function Z (ω) to be represented by a parallel combination of a resistance R_{ct} and a capacitance C_{dl}, both in series with another resistance R_s [27]:

$$Z(\omega) = R_s + \frac{1}{1/R_{ct} + i\omega C_{dl}} \qquad (2)$$

$\omega$is the frequency in rad/s, x = 2πf and f is frequency in Hz. To obtain a satisfactory impedance simulation of steel, it is necessary to replace the capacitor (C_{dl}) with a constant phase element (CPE) in the equivalent circuit. The most widely accepted explanation for the presence of CPE behavior and depressed semicircles on solid electrodes is microscopic roughness, causing an inhomogeneous distribution in the solution resistance as well as in the double-layer capacitance [28]. Constant phase element CPE$_{dl}$, Rs and R$_{ct}$can be corresponded to double layer capacitance, solution resistance, and charge transfer resistance respectively. To corroborate the equivalent circuit, the experimental data are fitted to equivalent circuit and the circuit elements are obtained.
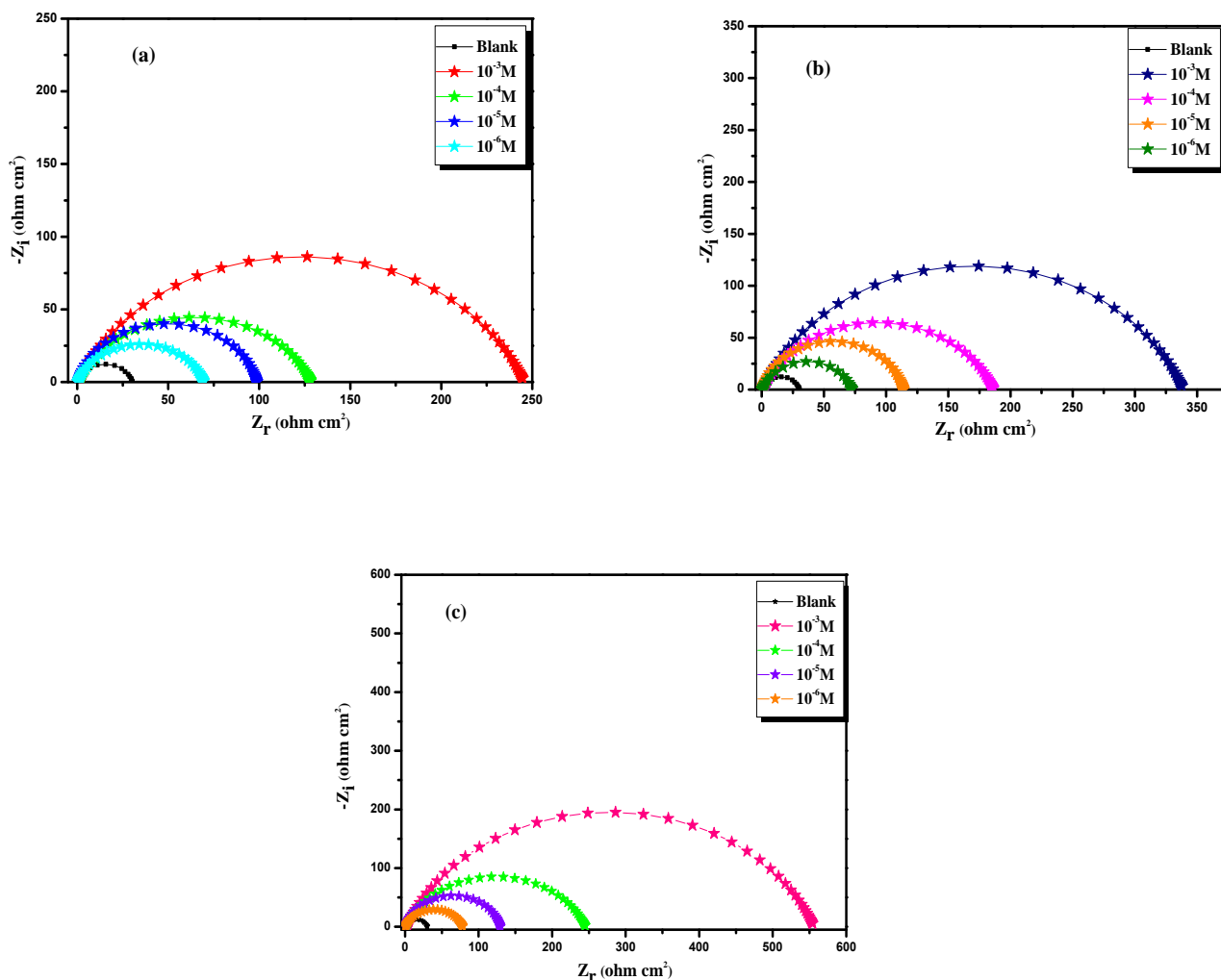
Fig.2. Nyquist curves for mild steel in 1.0MHClfor selected concentrations of the inhibitors: (a) 4-CBAT, (b) 3-CBAT, (c) 2-CBAT 303K.
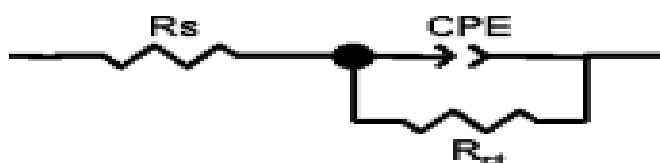
Figure3. Equivalent electrical circuit corresponding to the corrosion process on the carbon steel in hydrochloric acid.

Table 3 illustrates the equivalent circuit parameters for the impedance spectra of corrosion of steel in 1.0M HCl solution. The results demonstrate that the presence of inhibitors enhance the value of R_{ct} obtained in the pure medium while that of C_{dl} is reduced. The decrease in C_{dl} values was caused by adsorption of inhibitors indicating that the exposed area decreased. On the other hand, a decrease in C_{dl}, which can result from a decrease in local dielectric constant and/or an increase in the thickness of the electrical double layer, suggests that Schiff base inhibitors act by adsorption at the metal solution interface.

As the C_{dl} exponent (n) is a measure of the surface heterogeneity, values of (n) indicates that the steel surface becomes more and more homogeneous as the concentration of inhibitors increases as a result of its adsorption on the steel surface and corrosion inhibition. The increase in values of R_{ct} and the decrease in values of C_{dl} with increasing the concentration also indicate that Schiff bases act as primary interface inhibitors and the charge transfer controls the corrosion of steel under the open circuit conditions.
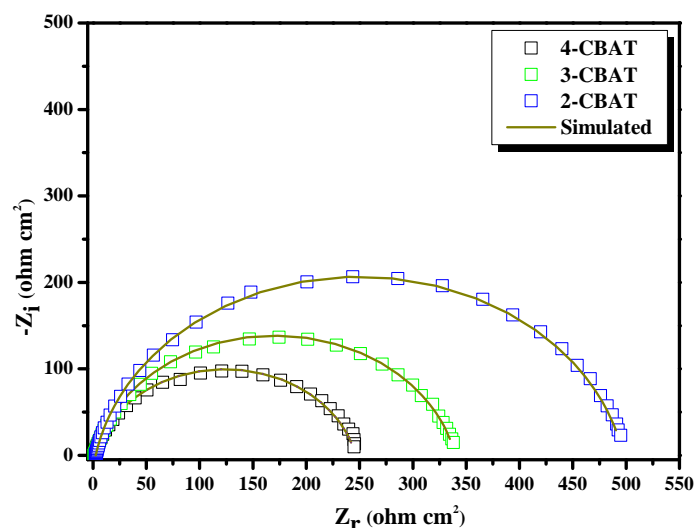
Figure4. EIS Nyquist plots for carbon steel in 1.0 M HCl with 1×10^{-3}M of inhibitors interface: dotted lines experimental data; dashed line calculated.

Table3. Electrochemical Impedance parameters for corrosion of carbon steel in acid medium at various concentrations of Schiff bases inhibitors.

Inhibitor	Conc (M)	R_S ($\Omega.cm^2$)	R_{ct} ($\Omega\ cm^2$)	n	CPE-T/$Y_0 \times10^{-5}$ ($s^n/\Omega\ cm^2$)	C_{dl} ($\mu F.cm^2$)	η_z (%)
Blank	1.0	----	29.35	0.87	17.61	80.22	-----
4-CBAT	10^{-3}	0.67	**245**	0.90	6.3180	40.15	**88.02**
	10^{-4}	0.41	128.22	0.90	8.1788	49.67	77.11
	10^{-5}	0.46	98.33	0.91	8.5911	55.21	70.15
	10^{-6}	0.37	69.29	0.85	16.287	73.06	57.15
3-CBAT	10^{-3}	0.93	**338.13**	0.95	4.5777	36.28	**91.32**
	10^{-4}	0.59	185.88	0.94	5.6417	44.34	84.21
	10^{-5}	0.53	113.36	0.91	7.4521	47.16	74.11
	10^{-6}	0.38	72.24	0.83	15.622	63.42	59.37
2-CBAT	10^{-3}	1.52	**495.00**	0.96	3.7898	32.74	**94.07**
	10^{-4}	0.79	310.30	0.95	4.2805	35.39	88.02
	10^{-5}	0.59	132.00	0.83	6.5481	46.17	77.25
	10^{-6}	0.41	50.87	0.94	14.453	56.35	62.41

3.3. Weight loss study

The corrosion rate (C_R) of carbon steel specimens after 6 h exposure to 1.0M HCl solution with and without the addition of various concentrations of the investigated inhibitor n-CBAT was calculated and the obtained data are listed in Table 4. The variation of C_R with inhibitor concentrations is shown in Fig. 5.The mean corrosion rate C_R (mg cm^{-2} h^{-1}), [29] and inhibition efficiency η_w of each concentration were calculated using the following equation [30]:

$$C_R = \frac{\Delta W}{St} \qquad (3)$$

$$\eta_w = \frac{C_R - C_{R(inh)}}{C_R} \times 100 \qquad (4)$$

Where ΔW is the average weight loss (mg), S is the area of the metal specimen in (cm^2), and t is the immersion time in hours (h), C_R and $C_{R\ (inh)}$ are corrosion rates in the absence and presence of inhibitors, respectively.

Fig.5 shows that the carbon steel corrosion rate was greatly reduced on the addition of inhibitors concentration, while inhibition efficiency η_w increased. This could be due to the fact that the inhibitor molecules act by adsorption on the steel/hydrochloric acid solution interface [31] Indeed, the adsorption of the Schiff base inhibitors could occur due to the formation of links between the d-orbital of iron atoms, involving the displacement of water molecules from the metal surface, and the lone sp^2 electron pairs present on the N atoms.

**Table4.** Effect of **n-CBAT** inhibitors concentration on corrosion data of carbon steel in 1.0 M HCl.

| Inhibitors	Concentration (M)	C_R (mg cm^{-2} h^{-1})	η_w (%)	Θ
Blank	1.0	1.135	---	---
4-CBAT	10^{-3}	0.1525	**86.57**	**0.8657**
	10^{-4}	0.3043	73.19	0.7319
	10^{-5}	0.3776	66.74	0.6674
	10^{-6}	0.5255	53.71	0.5371
3-CBAT	10^{-3}	0.1159	**89.78**	**0.8978**
	10^{-4}	0.2136	81.18	0. 8118
	10^{-5}	0.3171	72.06	0.7206
	10^{-6}	0.5019	55.78	0.5578
2-CBAT	10^{-3}	0.0744	**93.45**	**0.9345**
	10^{-4}	0.1531	86.52	0.8652
	10^{-5}	0.2756	75.72	0.7572
	10^{-6}	0.4447	60.82	0.6082
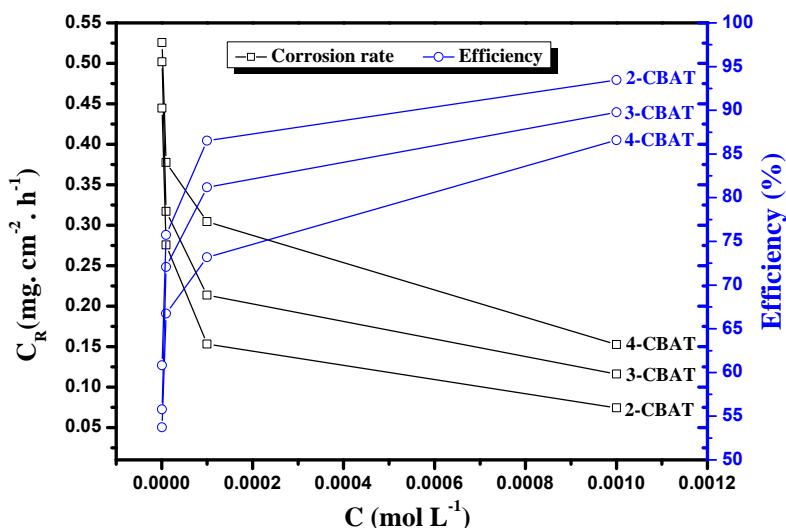
Figure 5: Relationship between the inhibition efficiency, corrosion rate and n-CBAT inhibitor concentrations for carbon steel after 6 h immersion in 1.0 M HCl at 303 K.

3.4. Effect of temperature

In order to investigate the inhibitive performance of n-CBAT derivatives affected by temperature, potentiodynamic polarization measurements were performed at various temperatures, ranging from 30 to 60°C, with and without 10^{-3}M of the Schiff base inhibitors. (Fig 6 and Figs7a-c). The results are given in Table 5.
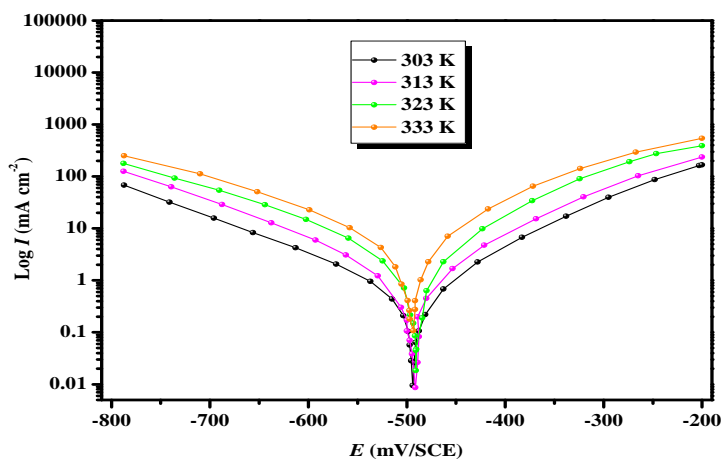
Figure 6: Potentiodynamic polarization curves of carbon steel in 1.0 M HCl at different temperatures.
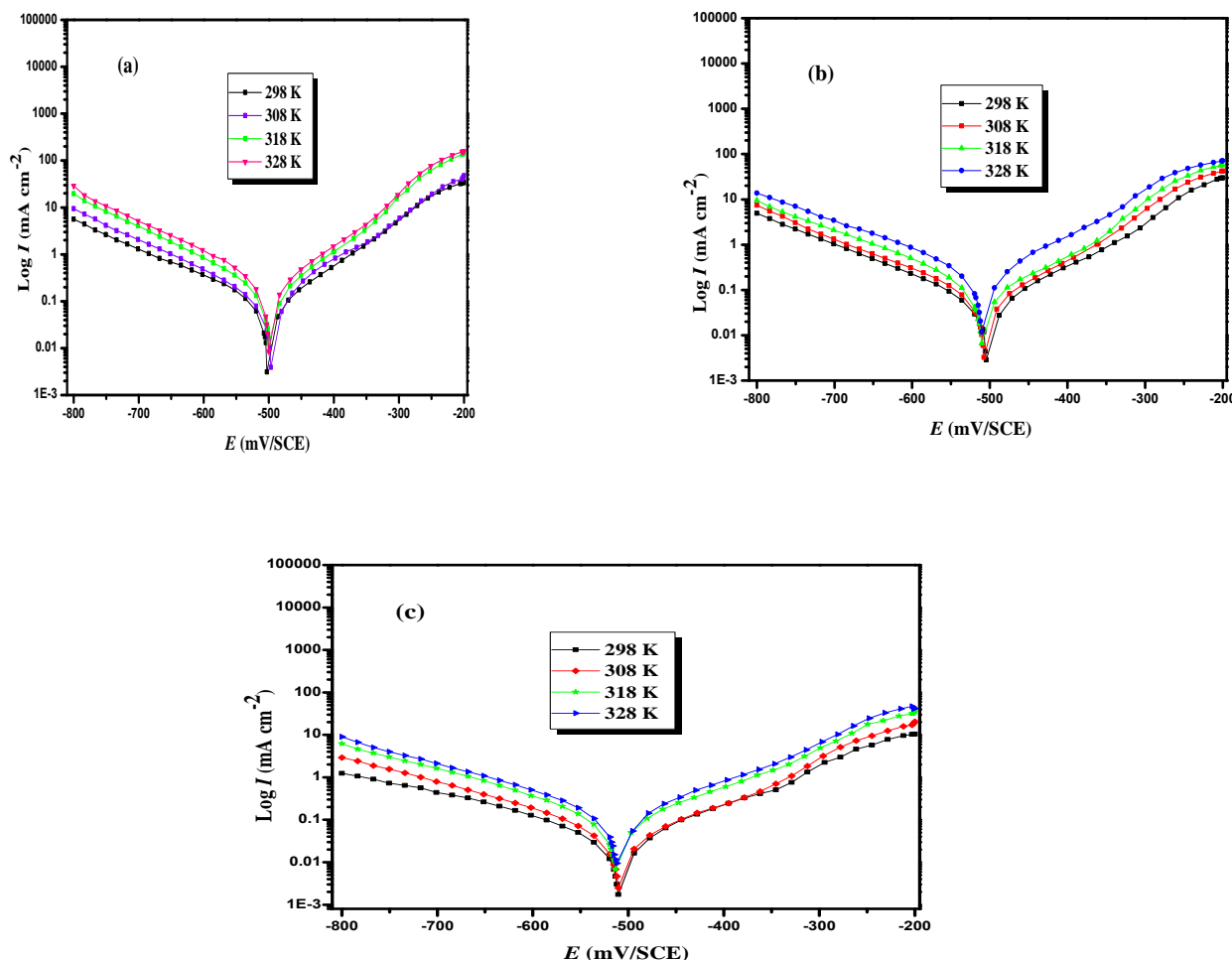
Fig.7. Potentiodynamicpolarisation curves of carbon steel in 1.0MHClfor various temperatures of the Schiff bases inhibitors: (a) 4-CBAT, (b) 3-CBAT, (c) 2-CBAT at 10^{-3} M.

Consequently, the activation energy (E_a), the enthalpy of activation (ΔH_a) and the entropy of activation (ΔS_a) for the corrosion of mild steel in 1.0M HCl in the absence and presence 10^{-3}M of the Schiff base inhibitors are calculated using Arrhenius equation [32,33] and transition state equation [34-36], respectively:

$$I_{corr} = k \exp\left(-\frac{E_a}{RT}\right) \tag{5}$$

$$I_{corr} = \frac{RT}{Nh} \exp\left(\frac{\Delta S_a}{R}\right) \exp\left(\frac{\Delta H_a}{RT}\right) \tag{6}$$

Where I_{corr} is corrosion current density, k is the Arrhenius pre exponential factor, R is the gas constant, h is the Planck's constant and N is Avogadro's number. According to the data in Table6, the plots of $\ln i_{corr}$ versus $1/T$ (Fig.8) and $\ln(i_{corr}/T)$ versus $1/T$ (Fig.9) show almost straight lines and all the regression coefficients are close to1. From the slopes and intercepts of the straight lines, the values of E_a, ΔH_a andΔS_a were calculated and listed in Table6.

Table5. Various corrosion parameters for Carbon steel in 1.0M HCl in absence and presence of optimum concentration of **n-CBAT** derivatives at different temperatures.

Inhibitor	Conc (M)	$-E_{corr}$ (mV/SCE)	$-\beta c$ (mV dec^{-1})	I_{corr} (mA cm^{-2})	η_{Tafel} (%)
Blank	303	496	162.5	564	--------
	313	498	154.5	773	--------
	323	492	176	1244	--------
	333	497	192	1650	--------
4-CBAT	303	503	155.4	**80.42**	85.74
	313	495	166.1	121.52	84.28
	323	509	158.7	198.79	84.02
	333	502	158.5	270.27	83.62
3-CBAT	303	515	160.6	**55.05**	90.24
	313	497	171.9	80.16	89.63
	323	509	158.7	137.46	88.95
	333	495	162.6	194.37	88.22
2-CBAT	303	511	157.1	**24.03**	95.74
	313	513	140.8	33.86	95.62
	323	498	157.3	57.85	95.35
	333	519	139.3	85.31.	94.83
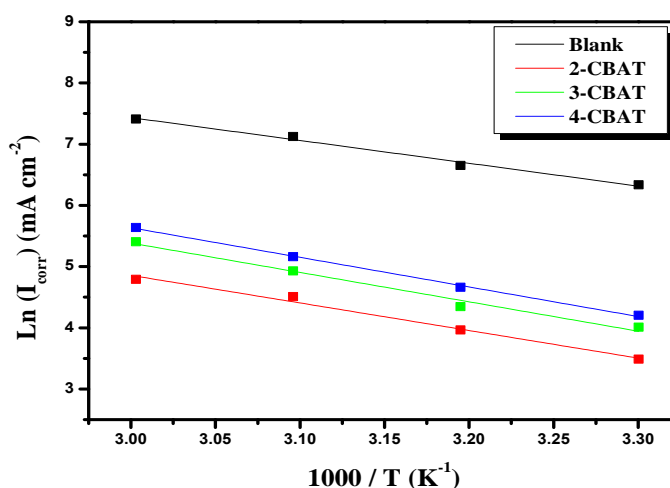
Fig.8. Arrhenius plots for mild steel in 1.0 M HCl and 1.0 M HCl + 10^{-3}M **n-CBAT** derivatives.

As seen from Table 5 and Fig.7a-c, it is apparent that the corrosion current densities increase in both uninhibited and inhibited solutions and the values of inhibition efficiency of **n-CBAT** were nearly constant in the temperature range studied (table 5). The corrosion current densities for carbon steel increased more rapidly with temperature in the absence of inhibitor (blank). These result confirmed that **n-CBAT** acts as an efficient inhibitors in the temperature range studied. The **n-CBAT** inhibitors efficiency was temperature-independent [37]. The value of E_a determined in the inhibited solutions is higher than that for uninhibited

578

solution ($31.00 kJmol^{-1}$), which indicates that a physical (electrostatic) adsorption occurs in the first stage [[32], [38], [36], [39].]. Besides, the increase in E_a can be correlated with the increase in the thickness of the double layer [38]. However, the adsorption process could not be classified as purely physical or chemical. Due to competitive adsorption with water molecules, the criteria of adsorption type obtained from the change of activation energy cannot be taken as a decisive.
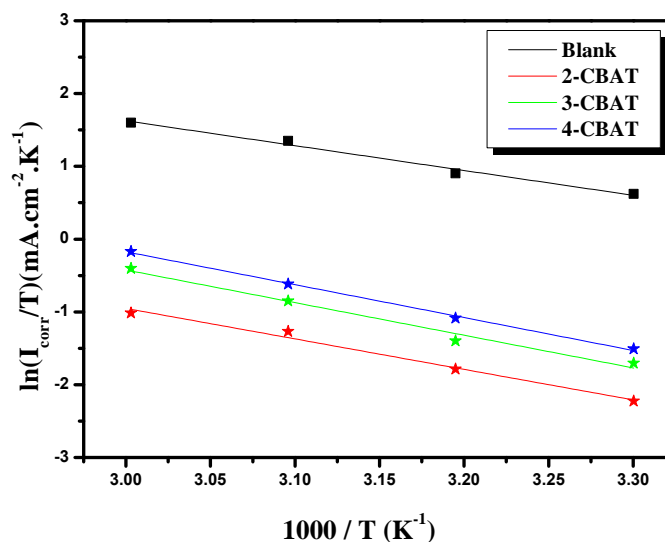
Fig9. Transition state plots for mild steel in 1.0 M HCl and 1.0 M HCl + 10^{-3}M **n-CBAT** derivatives.

Table6. Effect of temperature on Activation parameters of the corrosion in 1.0 M HCl in the absence andpresence of **n-CBAT** derivatives.

Concentration (M)	R^2	E_a (kJ mol^{-1})	ΔH_a (kJ mol^{-1})	ΔS_a (J mol^{-1} K^{-1})	E_a-ΔH_a (kJ mol^{-1})
Blank	0.995	31.00	28.35	-98.80	2.65
4-CBAT	0.985	40.22	37.58	-86	2.64
3-CBAT	0.979	39.91	37.27	-89	2.64
2-CBAT	0.997	37.47	34.83	-100	2.64

Therefore, the adsorption of **n-CBAT** molecules on the mild steel surface from HCl solution takes place through both physical and chemical processes simultaneously with predominantly first one [40]. Inspection of Table 6 revealed that the values of E_a andΔH_a are nearly the same, which should ideally be equal for a chemical reaction in electrolytic solutions [39]. The values ofΔS_a andΔH_a of mild steel in the presence of **n-CBAT** molecules are higher than that in the absence of **n-CBAT**. The positive sign of ΔH_a reflects the endothermic nature of the mild steel dissolution process [41]. whereas High and negative values of ΔS_a indicate the transition state complex which determines the reaction rate tends to associations rather than dissolutions, *i.e.*, the formation of activated complex causes the decrease in the disordering of transition process[42].

3.5. Adsorption isotherm

Organic inhibitors exhibit inhibition ability via adsorption on the solution/metal interface, while the adsorption isotherm can provide the basic information about the interaction between the inhibitor and the

metal surface [34, 43]. We tested various adsorption isotherms to fit the experimental data, such as Langmuir, Temkin, Flory–Huggins and Frumkin adsorption isotherms. For **n-CBAT** molecules, the plot of C versus C/θ yields a straight line with slope nearly 1 and the linear association coefficient (R^2) is also nearly 1 (Fig.10), showing that the adsorption of **n-CBAT** on the mild steel surface can be well described by Langmuir adsorption isotherm : Eq.(7). This kind of isotherm involves the single layer adsorption characteristic and no interaction between the adsorbed inhibitor molecules on the mild steel surface [44, 45].

$$\frac{C_{inh}}{\theta} = \frac{1}{K_{ads}} + C_{inh} \qquad (7)$$

Where C is the concentration of inhibitor in the electrolyte, K_{ads} is the equilibrium constant and θ is the surface coverage, calculated according to the following equation:

$$\theta = \frac{C_R - C_{R(inh)}}{C_R} \qquad (8)$$

The value of K_{ads} can be calculated from the intercept of the straight line and the standard free energy of adsorption (ΔG^0_{ads}) is estimated by Eq. (9):

$$\Delta G^0_{ads} = -RT \, Ln \, (55.5 K_{ads}) \qquad (9)$$

Where R is the gas constant, $Jmol^{-1}K^{-1}$ and T is the absolute temperature, K.
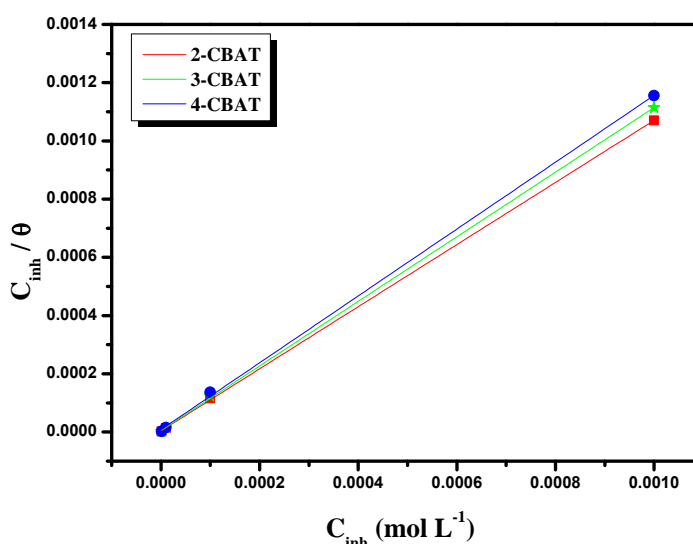
Figure10. Langmuir adsorption plot of **n-CBAT** compounds on mild steel in 1.0 M HCl with at 303K.

The value of ΔG^0_{ads} (Table7), indicating a strong interaction between the studied inhibitors and the mild steel surface in 1.0 M HCl solution [34]. The adsorption process of organic inhibitor molecules occurs as a result of replacement of water molecules previously adsorbed on the metallic surface. It can be assumed that the adsorption of **n-CBAT** derivatives on mild steel surface occurs first due to electrostatic interaction, and then desorption of water molecules is accompanied by chemical interaction between the adsorbate and metal surface [32, 33]. Two modes of adsorption can be considered: (**n-CBAT**) molecules are adsorbed on the steel surface due to the free electron pairs on the sulfur and nitrogen atoms as well as π-electrons of the aromatic rings. In acid media, (**n-CBAT**) exists in the form of protonated species (figure 11). If it is assumed that Cl⁻ anion are first is first adsorbed onto the metal, the adsorption of the cationic species would be limited by the surface concentration of anions, the neutral species being adsorbed when possible on free

surface sites [46]. So the triazole heterocycle may adsorb through electrostatic interactions between the positively charged molecules and negatively charged metal surface. It has been observed that the adsorption ammonium compounds can be influenced by the nature of anions [47, 48].

Table7. Thermodynamic parameters for the adsorption of inhibitors on the mild steel in 1.0 M Cl.at 303K

inhibitor	Slope	K_{ads} (M^{-1})	R^2	ΔG^0_{ads}
4-CBAT	1.15	1.2137×10^5	0.9996	-39.61
3-CBAT	1.11	2.0009×10^5	0.9999	-40.87
2-CBAT	1.07	2.6009×10^5	0.9999	-41.53

The specific adsorption of anions having a smaller degree of hydration such as chloride ions is expected to be more pronounced. Being specifically adsorbed, they create an excess negative charge towards the solution and favor more adsorption of the cations [49].

Figure11. Withdrawing effect of traizole heterocycle in **(n-CBAT)** molecules

4. Conclusion

Effect of chlorine group position on adsorption behavior and corrosion inhibition of (Chlorobenzylideneamino)-5-methyl-2,4-dihydro-1,2,4-triazole-3-thione **(n-CBAT)** Schiff base has been studied on carbon steel electrode in 1.0 M HCl by using weight loss and electrochemical techniques. Comparative study of these inhibitors shows that the inhibition efficiency follows the order: **4-CBAT <3-CBAT <2-CBAT**and the order of protection effect is the same for both weight loss and electrochemical. Impedance measurements indicate that with increasing inhibitors concentration, the polarization resistance (R_{ct}) increased, while the double layer capacitance (C_{dl}) decreased. Besides, the results of potentiodynamic polarization measurements also reveal that **(n-CBAT)** is a mixed type inhibitor, suppressing both anodic metal dissolution and cathodic hydrogen evolution reactions. Adsorption models: Langmuir, Temkin and Frunkin isotherms were tested graphically for the data and the best fit was obtained with the Langmuir isotherm. The variation in the protection ability of three Schiff bases can be attributed to their spatial molecular structure and molecular electronic structure.

References

[1] I. Ahamad, R. Prasad, M.A. Quraishi, Corros. Sci,vol. 52, p.933. 2010

[2] S. Issaadi, T. Douadi, A. Zouaoui, S. Chafaa, M.A. Khan, G. Bouet, Corros. Sci,vol. 53, p.1484. 2011

[3] R. Solmaz, Corros.Sci, vol. 52, p. 3321.2010

[4] I. Ahamad, Mater. Chem. Phys, vol.124, p. 1155.2010

[5] P. Lowmunkhong, D. Ungthararak, P. Sutthivaiyakit, Corros.Sci, vol.52, p. 30.2010

[6] K.C. Emregu, E. Duzgun, O. Atakol, Corros.Sci, vol.48, p. 3243.2006

[7]Stoyanova, A.E., Peyerimhoff, S.D. Electrochim. Acta, vol.47, p. 1365-1371.2002

[8]Valdez, L.M.R., Villafane, A.M., Mitnik, D.G. J. Mol. Struct. Theochem, vol.716, p. 61-65.2005

[9]B. Gomez, N.V. Likhanova, M.A.D. Aguilar, R.M. Palou, A. Vela, J.L. Gazquez, J. Phys. Chem. B, vol.18, p. 8928–8934.2006

[10]M. Finšgar, A. Lesar, A. Kokalj, I. Milošev.Electrochim. Acta, vol.53, p. 8287-8297.2008

[11] M. Gopiraman, N. Selvakumaran, D. Kesavan, R. Karvembu, Prog. Org. Coat, vol.73, p. 104. 2012

[12] H.M. Abd El-Lateef, dx.doi.org/10.1016./J.corsci.2014.11.040

[13] M. Lashgari, M.R. Arshadi, S. Miandari, Electrochim. Acta, vol.55, p. 6058.2010

[14] A. OngunYuce, G. Kardas, Corros. Sci, vol.58, p. 86.2012

[15] S. Issaadi, T. Douadi, A. Zouaoui, S. Chafaa, M.A. Khan, G. Bouet, Corros. Sci, vol.53, p.1484. 2011

[16] M.A. Migahed, Ahmed A. Farag, S.M. Elsaed, R. Kamal, H. Abd El-bary, Chem. Eng. Commun, vol.199, p. 1335.2012

[17] I. Ahamad, R. Prasad, M.A. Quraishi, Mater. Chem. Phys, vol.124, p. 1155.2010

[18] H.A. Mohamed, A.A. Farag, B.M. Badran, J. Appl. Poly. Sci, vol.117, p. 1270.2010

[19] S. Safak, B. Duran, A. Yurt, G. Turkoglu, Corros. Sci, vol.54, p. 251.2012

[20] K.C. Emregul, O. Atakol, Mater. Chem. Phys, vol.83, p. 373.2004

[21]Bouklah M., Benchat N., Aouniti A., Hammouti B., Benkaddour M., Lagrenée M., Vezin H., Bentiss F., Prog. Org. Coat, vol. 51, p. 118-124.2004

[22]N.A. Negm, Y.M. Elkholy, M.K. Zahran, S.M. Tawfik, Corros. Sci, vol.52, p. 3523.2010

[23]N.A. Negm, F.M. Ghuiba, S.M. Tawfik, Corros. Sci, vol.53, p. 3566.2011

[24]Ferreira, E.S., Giancomelli, C., Giacomelli, F.C., Spinelli, A, Mater. Chem. Phys, vol.83, p. 129-134.2004

[25]M.A. Hegazy, Corros. Sci, vol.51, p. 2610.2009

[26] K. Mallaiya, R. Subramaniam, S.S. Srikandan, Electrochim. Acta, vol.56, p.3857.2011

[27] I. Danaee, J. Electroanal. Chem, vol.662, p. 415.2011

[28] I. Danaee, S. Noori, Int. J. Hydrogen Energy, vol.36, p. 12102.2011

[29] Bincy Joseph, Sam John, K.K. Aravindakshan, Abraham Joseph, Indian J. Chem. Technol, vol.17, p. 425-430.2010

[30] Bin Xu, Ying Liu, Xiaoshuang Yin, Wenzhong Yang, Yizhong Chen, Corros. Sci, vol.74, p. 206-

213.2013

[31] S.S. Abd El-Rehim, M.A.M. Ibrahim, K.F. Khaled, J. Appl. Electrochem, vol.29, p.593.1999

[32]Xu B, Liu Y, Yin XS, Yang WZ, Chen YZ, Corros Sci, vol.74, p.206–13.2013

[33]Xu B, Yang WZ, LiuY, Yin XS, Gong WN, Chen YZ, Corros Sci, vol. 78, p.260–8.2014

[34]Zheng XW, Zhang ST, Li WP, Yin LL, He JH, Wu JF, Corros Sci, vol. 80, p.383–92.2014

[35]Hegazy MA, El-Tabei AS, Bedair AH, Sadeq MA, Corros Sci, vol. 54, p.21930.2012

[36]Yadav DK, Quraishi MA, Maiti B, Corros Sci, vol. 55, p. 254–66.2012

[37] Tang YM, Zhang F, Hu SX, Cao ZY, Wu ZL, Jing WH, CorrosSci, vol. 74. 271–82.2013

[38]Solmaz R, Karda¸ sG , Çulha M, Yazıcı B, Erbil M, Electrochim Acta, vol. 53, p. 5941–52.2008

[39] Singh AK, Quraishi MA, CorrosSci, vol. 52, p.1529–35.2010

[40]Solmaz R, CorrosSci, vol. 79, p. 169–76.2014

[41] N.M. Guan, L. Xueming, L. Fei, Mater. Chem. Phys, vol. 86, p. 59.2004

[42] S. Martinez, I. Stern, Appl. Surf. Sci, vol. 199, p. 83.2002

[43]Musa AY, Kadhum AAH, Mohamad AB, Takriff MS, Corros Sci, vol. 52, p.3331–40.2010.

[44]Outirite M, Lagrenée M, Lebrini M, Traisnel M, Jama C, Vezin H, et al, Electrochim Acta, vol. 55, p.1670–81. 2010

[45]Elayyachy M, Idrissi AE, Hammouti B, CorrosSci, vol. 48, p.2470–9.2006

[46].E. Blomgren, J.O'M. Bockris, J.Phy.Chem. 63(1959)1475

[47].S. Rengamani, S. Muralidharan, M. Anbu Kulandainathan, S. Venkatakrishna Iyer, J. Appl. Electrochem, vol.24, p. 355.1994

[48].Z. A. Foroulis, Proceeding of the sixth European Symposium on corrosion, Ferrara, vol.8, p.130.1985

[49].Z.A.Iofa, G.N. Thomashov, Zh. Fis. Khim, vol.34, p. 1036.1960